Oil dispersal modelling: reanalysis of the Rena oil spill using open-source modelling tools

HFE Jones, MTS Poot, JC Mullarney, WP de Lange & KR Bryan

Taylor & Francis
Taylor & Francis Group

RESEARCH ARTICLE

Oil dispersal modelling: reanalysis of the *Rena* oil spill using open-source modelling tools

HFE Jones[a,b], MTS Poot[b], JC Mullarney[b], WP de Lange[b] and KR Bryan[b]

[a]Waikato Regional Council, Hamilton, New Zealand; [b]Coastal Marine Group, School of Science, University of Waikato, Hamilton, New Zealand

ABSTRACT

Oil spill forecast modelling is typically used immediately after a spill to predict oil dispersal and promote mobilisation of more effective response operations. The aim of this work was to map oil dispersal after the grounding of the MV *Rena* on Astrolabe Reef and to verify the results against observations. Model predictions were broadly consistent with observed distribution of oil contamination. However, some hot spots of oil accumulation, likely due to surf-zone and rip current circulation, were not well represented. Additionally, the model was run with 81 differing wind conditions to show that the events occurring during the grounding represented the typical likely behaviour of an oil spill on Astrolabe Reef. Oil dispersal was highly dependent on prevailing wind patterns; more accurate prediction would require better observations of local wind patterns. However, comparison of predictions with observations indicated that the GNOME model was an effective low-cost approach.

Introduction

On 5 October 2011 a 47,000 tonne container ship, the MV *Rena*, ran aground on the Astrolabe Reef (37.540°S, 176.425°E) on the approach to Tauranga harbour (Figure 1). There were 1733 tonnes of oil on board the *Rena*, of which 1300 tonnes were recovered before 4 May 2012 (source: Maritime New Zealand). During the week after the grounding, approximately 350 tonnes of heavy fuel oil were released on to the shelf, where the oil was subjected to tidal currents, wind-induced currents and shelf currents, which advected and dispersed the oil, with a large fraction stranding on Waihi beach, Matakana Island, Mount Maunganui beach, Papamoa beach, and lesser amounts being dispersed farther afield (Schiel et al. 2016). A small fraction entered Tauranga harbour and Maketu estuary.

A number of institutions provided oil spill response forecast modelling immediately after the *Rena* grounding to guide response operations. However, there was no formal quantitative verification of the predictions provided by the models; accurate predictions require careful model calibration and verification against observations of currents, oil dispersal and shoreline accumulation and the necessary data were not available during the response. The aim of this study was to use freely available open-source modelling tools to hindcast the oil dispersal after the *Rena* grounding, to verify the results against
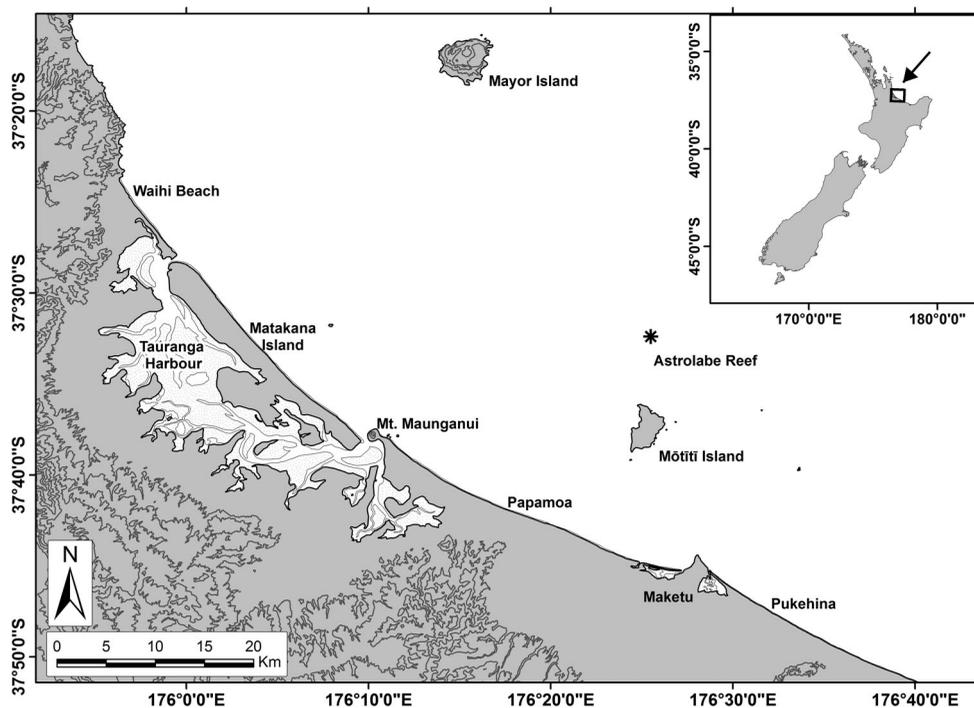
Figure 1. Tauranga harbour and Bay of Plenty coastline. Location of the *Rena* grounding, Astrolabe Reef, marked with an asterisk.

information on oil accumulation collected by Maritime New Zealand and to use multiple model simulations to provide a preliminary hazard map, from which an understanding of the most common oil dispersal patterns associated with a grounding on Astrolabe Reef can be inferred. The advantage of open-source modelling systems is that there is a greater likelihood of multiple institutions using the same systems and so model set-up files and results can be easily exchanged between working groups allowing for greater collaboration, verification and quality control.

Methods

Astrolabe Reef is approximately 7 km north of Mōtītī Island and 24 km northeast of Mt Maunganui in the Bay of Plenty in the North Island of New Zealand (Figure 1). The Bay of Plenty coastline is a low-energy wave environment, sheltered from the prevailing westerly and southwesterly swell that affects other areas of New Zealand (Heath 1985; Gorman et al. 2003). Tides (at Tauranga) range between 1.62 m for spring tides and 1.24 m for neap tides. The tidal currents on the shelf are relatively weak (0.05–0.10 m s^{-1}), compared with wind-driven currents that reach 0.25 m s^{-1} (Black et al. 2005; Longdill et al. 2008).

Delft3D-FLOW, developed by Deltares and available as open-source software, is a hydrodynamic simulation program that calculates non-steady flow from tidal and meteorological forcing on a rectilinear or curvilinear boundary-fitted grid. Delft3D-FLOW may

be implemented in 3D, with the vertical grid defined using the sigma (σ) co-ordinate approach, or in 2D using a depth-averaged approach (2DH) (Deltares 2011). The model has been extensively validated (e.g. Elias et al. 2000; Lesser et al. 2004).

In this study, the Delft3D model domain included both the northern and southern basins of Tauranga harbour. The grid extended approximately 25 km offshore (to a water depth of around 70–90 m) and approximately 60 km along shore from Waihi to Maketu. The grid resolution was 200 × 200 m in the horizontal and the grid was rotated at an angle of 50° to the north-south axis (Figure 2). Bathymetry was derived from various sources, such as echo soundings and nautical charts (Kwoll 2010). The model was run in both 3D and 2D simulation modes. The 3D mode provided slightly more accurate results around the entrance to Tauranga harbour and so was used to simulate conditions around the October 2011 event. The 2D model was then used to run 81 different scenarios to assess the likely impact of spills occurring during other wind conditions. The 2D version was used for this rather than the 3D version because the minor difference in modelled open coast flow fields did not warrant the order of magnitude-larger run-times associated with the 3D model. The number and thickness of the layers in the 3D model were determined based on the need for fine resolution near the bed (to resolve the logarithmic profile of the horizontal velocity components in the vertical) and near the surface. Based on these considerations (and the need for the layer thickness to have a smooth distribution), the 3D model had 16 σ-layers, with layer thicknesses between the bed and the surface set to 1.5%, 2%, 2.8%, 4%, 5.6%, 7.8%, 11%, 15.3%, 15.3%, 11%, 7.8%, 5.6%, 4%, 2.8%, 2% and 1.5% of total depth.

Hydrodynamic simulations were forced at the open boundaries using the tidal constituents M2, N2, S2, K1, MU2, O1 and L2. Time series of water levels at the four corners of the open boundaries were derived from water levels predicted by the NIWA tidal model (http://www.niwa.co.nz/services/online-services/tide-forecaster), which also includes these constituents. Constituents were extracted from the water levels using the tidal harmonic analysis package, 't_tide' (Pawlowicz et al. 2002). Flow at the boundaries was forced using astronomic Riemann boundary conditions (3D model) or Neuman conditions
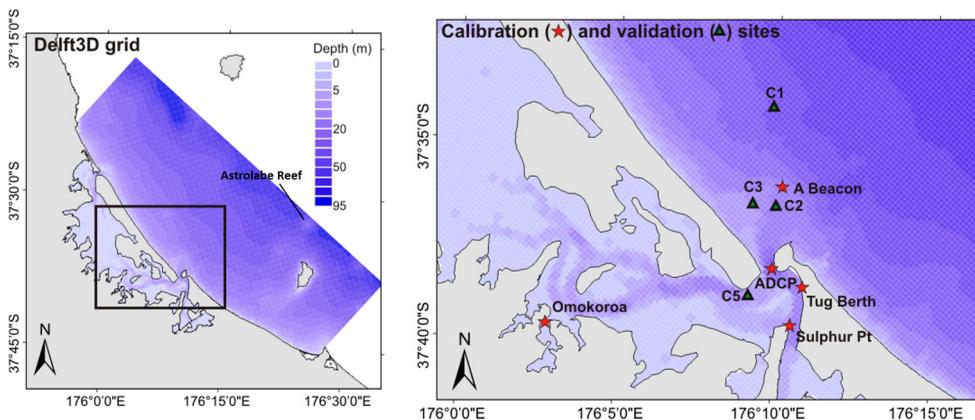

Figure 2. Delft3D model grid and location of calibration (star) and validation (triangle) sites.

(depth-averaged model) at the open boundaries. Riemann boundary conditions are based on a linearised Riemann invariant (F_R; m s^{-1}):

$$F_R = U + \eta\sqrt{\frac{g}{h}}$$

where, U is velocity, η is sea surface elevation, g is acceleration due to gravity and h is water depth. This type of boundary reduces reflection of obliquely incident waves and is non-reflective for outgoing waves normal to the boundary (e.g. Mullarney et al. 2008). Free slip (no shear stress) conditions were applied at the closed boundaries and the vertical velocity profile at the boundaries was a logarithmic function of the water depth.

Delft3D calibration and validation methods

The Delft3D-FLOW calibration simulation began on 1 October 2011 from a 'cold start' (i.e. uniform water levels, no currents) and ran for 30 days with a 60 s time step (3D model) and 15 s time step (2D model). To reduce numerical instabilities in the initial adjustment period, the boundary forcing was gradually applied over a smoothing period. Continuous measurements of tidal elevation were provided by Bay of Plenty Regional Council and Port of Tauranga for three stations inside the harbour—Omokoroa, Sulphur Point and Tug Berth—and one station outside the harbour, A Beacon (Figure 2). ADCP current meter data collected in the harbour entrance were also provided by the Port of Tauranga. The model was calibrated by adjusting parameters including the Chézy roughness coefficient, threshold depth and horizontal eddy viscosity. The model error was represented by model performance statistics: the coefficient of determination (R^2) and the mean absolute error (MAE). Model calibration is shown for the 3D version and similar results were obtained for the 2D version.

Parameters resulting from the Delft3D model calibration were fixed for a further month-long simulation for the purposes of model validation. Water level and current data collected at five sites inside and outside the harbour between 10 May and 10 June 2006, described in detail in Spiers et al. (2009), were used for model validation. Tidal elevation, current velocity and direction were measured at three sites outside (C1, C2 and C3) and one site inside (C5) Tauranga harbour (Figure 2). Station C4 was not used as it was found to contain erroneous data (Spiers et al. 2009).

Delft3D model calibration results

The Delft3D models were calibrated by adjusting the bottom roughness coefficient, threshold depth and horizontal eddy viscosity (Table 1). The final calibrated 3D-Chézy coefficient was spatially variable, ranging from 80–40 m$^{1/2}$ s^{-1} for the 3D model and 180–10 m$^{1/2}$ s^{-1} for the 2D model from shallow and deep water, corresponding to roughness lengths (z_0) that increased with depth and were broadly consistent with those provided in the literature for unrippled mud/sand and rippled sand (e.g. Soulsby 1997).

The Delft3D modelled and measured water levels for the stations used in model calibration and validation were in good agreement for both models (R^2 0.96–0.98, MAE 0.07–0.08 m for the 3D model, also provided in Table A1.1 and Figure 3 [thin dashed line, 3D model, thin solid line, 2D model]). The models predicted tidal amplitudes to

Table 1. Calibrated model parameters for the Delft3D models.

Parameter	Value	Units
Threshold depth	0.01	m
Horizontal eddy viscosity	10	$m^2\,s^{-1}$
Vertical eddy viscosity	0	$m^2\,s^{-1}$
Turbulence model	k-ε	
Number of layers (3D)	16	
Number of layers (2D)	1	
Chézy roughness coefficient (3D)	Spatially variable (80–40)	$m^{1/2}\,s^{-1}$
Chézy roughness coefficient (2D)	Spatially variable (180–10)	$m^{1/2}\,s^{-1}$

within 0.03 m and predicted tidal phases for the major tidal constituents (M2, N2 and S2) at sites outside Tauranga harbour and near the harbour entrance to within 5°. However, the models tended to under-predict the phase in the inner harbour (i.e. at Omokoroa) by approximately 6°–7° (Table A1.1).

For the calibration period, 3D modelled current velocities for the Delft3D model were consistently lower than those measured at the Port of Tauranga ADCP site (MAE 0.41 m s^{-1}; Table A1.2; Figure 3). This result was particularly true for the 2D model. However, the model did capture the pattern of higher ebb tide velocities, compared with flood, and modelled current directions compared well with measured data (MAE 18° for flood tide and 30° for the ebb).

Velocities at validation sites C1, C2 and C3 were also consistently lower than measured velocities (MAE 0.04–0.10 m s^{-1}, 52%–67% of the average measured current velocity), but
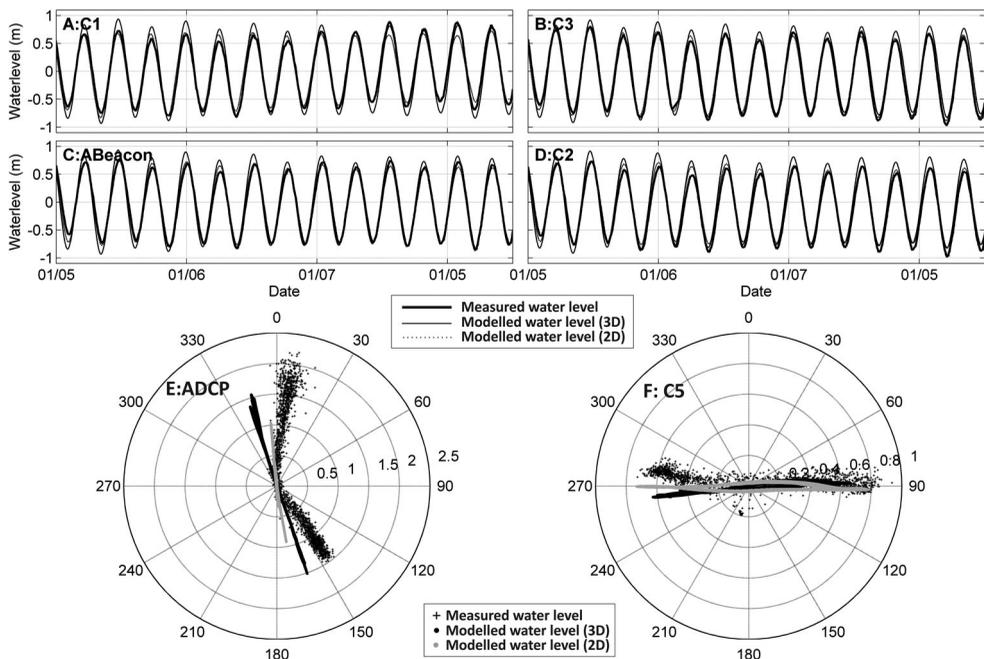

Figure 3. Measured and modelled water levels for validation sites **A**, C1; **B**, C3; **D**, C2, and calibration site **C**, A Beacon, and measured and modelled current velocity and direction for **E**, the calibration ADCP site and **F**, validation site C5.

were better predicted at site C5 (MAE 0.10 m s^{-1}, 22% of the average measured current velocity; Table A1.2; Figure 3). The current velocity MAE in the 2D version was lower than that of the 3D model both outside and inside the harbour, whereas the 3D version had lower MAE for flows around the complex entrance area. As with the ADCP (calibration) site, the models captured the pattern of higher ebb tide velocities at sites inside and near the harbour entrance (i.e. C2, C3 and C5; Table A1.2). Modelled current direction compared very well with measured data at site C5 (MAE ebb tide 3.5° and MAE flood tide 12.8° for the 3D model [with a slightly better fit for the 2D model; Figure 3]), with reasonable agreement between measured and modelled data for sites C1, C2 and C3 (MAE approximately 10°–14° for the 3D model and slightly more for the 2D model). Note that the calibration and verification sites were not established specifically for the purposes of this study and are clustered around the entrance, where the tidal currents are likely to be higher. It is possible that calibration/validation would not be as successful using observations in deeper water where shelf currents may be more important.

GNOME calibration and validation methods

GNOME (General NOAA Oil Modeling Environment) is a freely available oil spill trajectory model that simulates the movement of oil due to winds, surface currents and spreading (Zelenke et al. 2012). The spill trajectory includes both a 'best guess' and a 'minimum regret' solution that takes into account the uncertainty in the model inputs. GNOME is a two-dimensional Eulerian/Lagrangian model that requires three major inputs: maps, movers (current, wind or diffusion) and spills. The movement of the oil is calculated from the u (east–west) and v (north–south) velocity components, summed for all the movers at each time step, using a first-order Runge-Kutta method.

For this study, output from Delft3D for 5 October (i.e. when the *Rena* grounded) to 30 October 2011 was used as input in GNOME as a current mover. At present, GNOME can use only 2D currents, so in the case where the 3D model was used, surface flows from the Delft3D model output were used as input to GNOME. Maps for the western Bay of Plenty coastline were obtained from the GOODS (GNOME Online Oceanographic Data Server) map generator tool (http://gnome.orr.noaa.gov/goods). Hourly wind speed and direction were acquired from NIWA's CliFlo service (National Institute of Water and Atmospheric Research National Climate Database, http://cliflo.niwa.co.nz/) and applied spatially uniformly over the entire domain.

GNOME calculates the diffusion of oil (random spreading) using a simple random walk based on a diffusion value (representing horizontal eddy diffusivity and ranging from 0.1–100 m^2 s^{-1}). Oil spills can be modelled as up to 10,000 Lagrangian Elements (LEs), each of which have parameters assigned including location, release time, age, pollutant type and status (floating, beached, evaporated or off the map). Windage is the movement of oil by the wind, which is typically about 3% of the wind speed (Zelenke et al. 2012). Refloating in GNOME is determined by the refloat half-life, which is defined as the number of hours in which half of the oil that has beached is removed by an offshore wind, diffusion or raised water levels (such as an incoming tide). Additional parameters describe uncertainty in the wind, current and diffusion movers, and thus control the output for the minimum regret LEs.

In this study, the *Rena* spill was initialised using data from Maritime New Zealand that described the timing and amount of oil spilled from the vessel. Some of these data consisted of estimates obtained from mapping the approximate dimensions of the surface accumulation near the wreck from a helicopter. The uncertainty surrounding the release behaviour of the oil is an unfortunate but unavoidable limitation of this study (and represents a continuing challenge for modelling oil spills of this type). The *Rena* grounded at 0200 h on 5 October 2011 and approximately 350 tonnes of oil leaked from the ship (typically at low tide) between then and late October (Schiel et al. 2016). The majority of the oil likely leaked from the vessel between 10 and 12 October, when weather conditions were poor (winds speeds typically 5–8 m s^{-1}, from the north to northeasterly direction).

A verification database was collated from data on oil dispersal and accumulation after the *Rena* grounding, obtained from Maritime New Zealand in the form of SCAT (Shore Clean-up Assessment Techniques) survey reports and over-flight observations. Data were extracted and compiled to summarise critical information (where available), such as the survey/oil location, the beach zone surveyed (e.g. lower, middle or upper intertidal), the amount of oil observed (e.g. as percentage cover on the shoreline) and oil character (e. g. tar balls, tar patties).

From the SCAT data, two metrics were calculated for each day in October after the grounding: first, the average oil percentage cover (averaged across the intertidal zones for each location surveyed and averaged across all locations surveyed); and second, the maximum oil percentage cover. Data on the quantity of oil removed from the beaches was insufficient to estimate the actual amount (in tonnes) of oil accumulated on the shoreline, thus it was not possible to quantitatively compare GNOME output (tonnes of oil accumulated on the shoreline) with SCAT data (percentage cover of oil on the shoreline). However, GNOME output and SCAT data were compared to assess model accuracy with respect to the timing and location of oil accumulation. Additionally, maps of oil dispersal (in the water) and accumulation (on the shoreline) were provided by Maritime New Zealand that summarised the SCAT and over-flight observations, which were compared with GNOME model output.

The hazard associated with the *Rena* grounding was assessed by running 81 wind event scenarios over 21 days covering a spring and neap tide. The 81 events were chosen from the range of wind speeds and directions that were measured at Tauranga airport from 1995 to 2012. Note that the winds were maintained constant during the 3-week modelling period. (It was not possible to model unsteady wind conditions and include all combinations that were statistically likely to occur.)

GNOME model calibration results

The GNOME model was calibrated by adjusting parameters associated with diffusion, the refloat half-life, model time step, uncertainty and windage (Table 2). The refloat half-life was set at 12 h for the shelf model to reflect the (predominantly) sandy beaches on the open coastline (Dancuk 2009). Along- and cross-current uncertainty values were increased (compared with default values) due to the uncertainty around the current predictions by the Delft3D model.

The amount of oil released, floating, beached, evaporated and dispersed, and that which had moved out of the modelled area ('off map') was output from the model every 6 h for

Table 2. Calibrated model parameters for the GNOME model.

Parameter	Value	Units
Diffusion	1	$m^2 s^{-1}$
Diffusion uncertainty	1	
Refloat half-life	12	Hours
Time step	0.17	Hours
Windage	1–4	%
Wind speed scale	2	$m s^{-1}$
Wind angle scale	0.4	Radians
Along current uncertainty	25	%
Cross current uncertainty	25	%

the entire simulation (Figure 4A). The majority of the oil over most of the simulation remained floating; although a significant proportion (100 tonnes or approximately 35% of that released) evaporated or dispersed within a few days. The amount of oil beached on the shoreline averaged approximately 10% of the total released over the entire simulation (i.e. 5–30 October), although this peaked at 30% at 3 and 10 days after release. By the end of the simulation, approximately 40% of the oil had travelled outside the modelled area (mostly to the north and east). The amount of oil entering Tauranga harbour and Maketu estuary was relatively small (<5–10 tonnes).

Results

Comparison of GNOME output with observations

GNOME model output generally compared well with observations. The amount of oil beached across the entire model domain (the best estimate, not including the uncertainty solution) was output from the model every 6 h and visually compared with SCAT report data (Figure 4B). The GNOME model predicted that oil would first reach the shoreline on 11 October, and by 13 October large amounts of oil (about 60–90 tonnes) would have accumulated on the coastline. However, the model did not predict the arrival of the small amount of oil that was observed to reach the shoreline on 10 October. Although it was not possible to estimate the actual amount of oil that did accumulate on the shoreline based on SCAT reports that gave estimates of percentage cover, the observations do indicate that the maximum oiling did occur on 13 October, as predicted by the model (Figure 5). Further peaks in oil accumulation on 15–16 October and 19–20 October captured by the model also largely matched observations of maximum and average oil coverage on the shoreline.

The GNOME model indicated that oil entered Tauranga harbour (through the southern entrance) from a northeasterly direction between 10 and 13 October. The wind direction changed to northwesterly from 13 to 14 October and the majority of the oil began to move offshore. These model results are consistent with SCAT surveys that indicated presence of oil inside Tauranga harbour by 17 October (Figure 4B).

Preliminary hazard assessment

Wind data from Tauranga airport show that southwesterly winds with speeds of between 4 and 8 $m s^{-1}$ are the most common conditions around Tauranga (Figures 6 and 7A). Of the
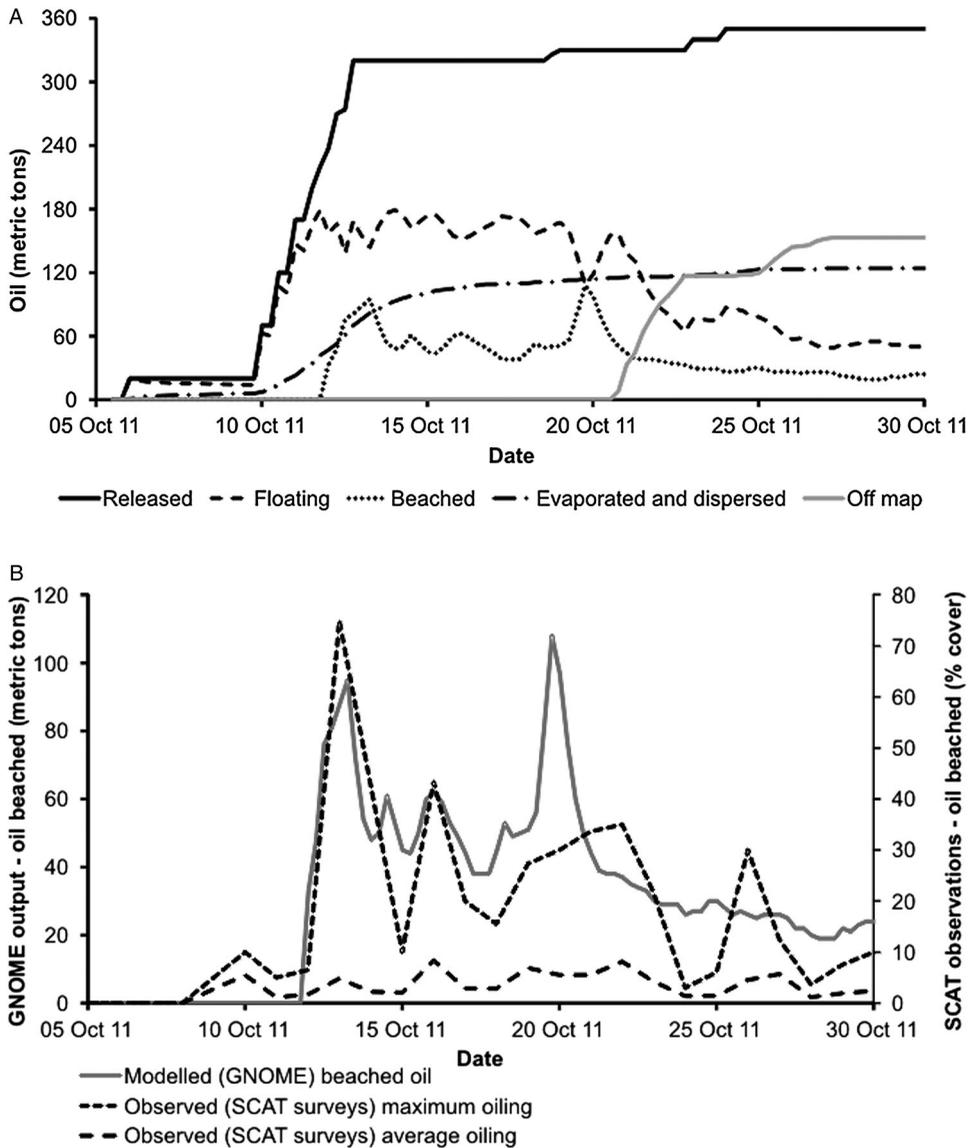
Figure 4. A, Amount of oil released from the *Rena*, floating, beached on the shoreline, evaporated and dispersed or 'off map' (i.e. outside of modelled area) throughout the duration of the GNOME simulation (5–30 October 2011). **B,** Modelled (GNOME) oil beached on the shoreline (in metric tons) and maximum and average oil percentage coverage as assessed by SCAT surveys.

most common wind speeds, winds from 220° were also associated with the longest arrival times of oil at the shoreline. Northeasterly winds were the wind patterns that caused the modelled oil spill to reach the coastline most quickly, with the largest wind events causing the fastest arrival times (Figure 7B) (although the probability of the large wind events occurring was very low). Northeasterly winds were associated with the great tonnage of accumulated oil at the shoreline over the 20-day modelling period (Figure 7C).
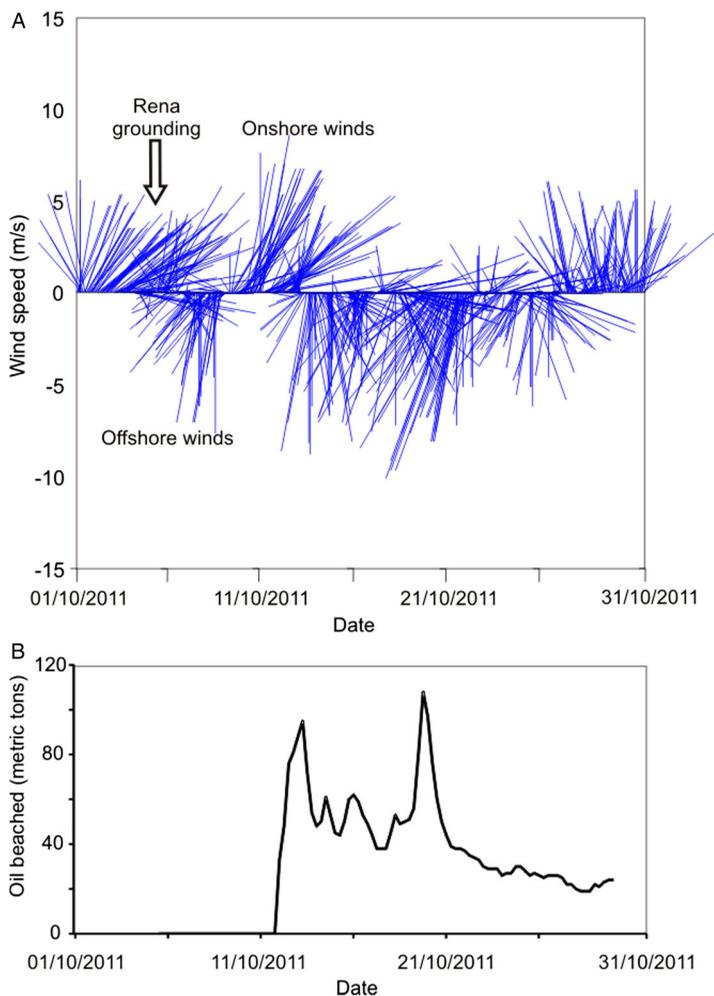
Figure 5. A, Wind speed and direction measured at Tauranga airport in October 2011, with time of *Rena* grounding indicated by the arrow. Positive values on y axis represent northerly winds, negative values represent southerly winds. For example, offshore (southerly to southwesterly) winds are evident from 6–8 October 2011. **B,** Modelled (GNOME) amount of oil beached on shoreline. Note peak in oil beached on shoreline 12–13 October after a period of onshore (northeasterly) winds, followed by a reduction in oil beached after moderate (>5 m s^{-1}) offshore (southerly) winds.

Discussion

GNOME model performance

The GNOME model compared well with observations (i.e. SCAT surveys), generally predicting the timing and location of oiling on the shoreline, peaks in oil accumulation and timing of the oil entry into Tauranga harbour. The qualitative nature of the observed data prevented quantitative comparison between model output and observed oil accumulation. More accurate measurement of the amount of oil that accumulated on shorelines could have improved GNOME model verification, but was not a priority during *Rena* oil spill clean-up response operations.
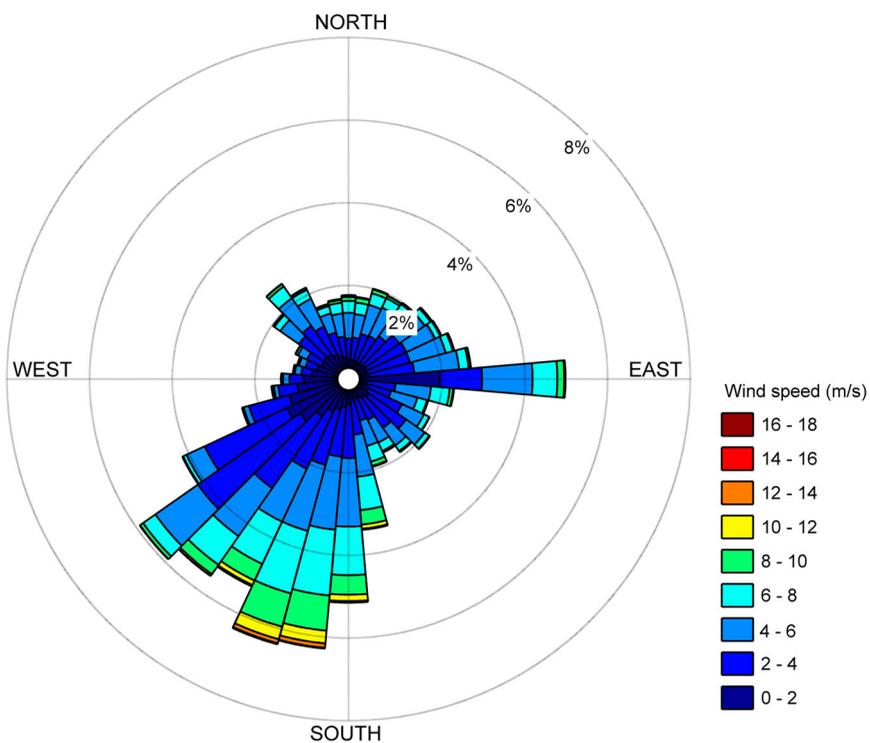
Figure 6. Wind speeds and directions measured at Tauranga airport from 1995 to 2012. Colours denote wind speed and the length of each radial bar reflects the probability of that wind condition occurring.

There was a slight discrepancy between the timing of the first instance of oil on the shoreline (10 October observed cf. 11 October modelled). However, there was uncertainty around the timing and amount of oil lost from the vessel in the days after the grounding (Maritime New Zealand 2011) and inaccurate initialisation of the oil spill in GNOME will affect the accuracy of the simulation results. When used in real-time operations (i.e. when used to forecast rather than hindcast), the oil spill amount and extent can be initialised and updated based on over-flight data (Zelenke et al. 2012), which should improve model predictions. The GNOME model appears to over-predict the oil beached on 19–20 October, but SCAT reports indicate that there was beach clean-up (i.e. removal of oil) in progress before and around this time. It was not possible to take removal of oil from beaches into account with the GNOME model due to uncertainty about the amount and location of oil removed, which may account for the over-prediction of oiling around this time.

The oil that did beach on the shoreline was not evenly dispersed, with 'hot spots' of accumulation evident in the model output and in SCAT observations, for example, at Papamoa beach, parts of the western shoreline of Mōtītī Island and Okurei Point (east of Maketu). Surf-zone rip currents are common along the sandy beaches of the Bay of Plenty coast (e.g. Stephens et al. 1999) and these can trap oil within their recirculation systems. SCAT observations indicate that the oiling along the coastline from Mt Maunganui to Maketu indeed had a patchy distribution. However, the model only includes the
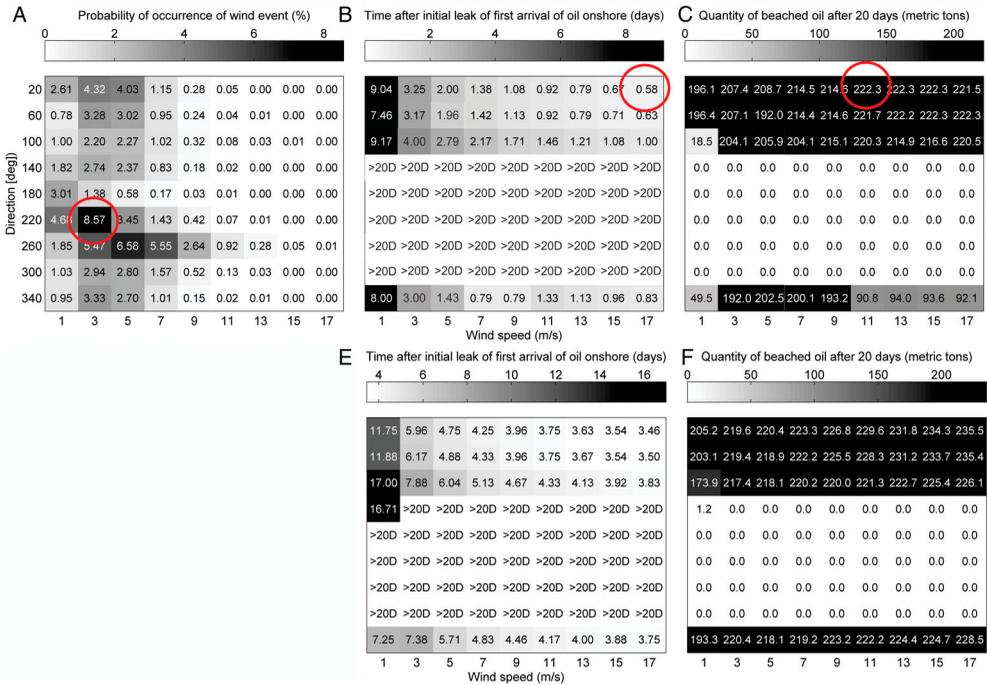
Figure 7. A, The proportion of wind speeds and directions measured at Tauranga airport from 1995 to 2012, split into 81 wind events. **B,** Modelled (GNOME) times after the initial oil leak for the first oil to be beached, for constant wind conditions. Simulations with no oil landing onshore within 20 days are labelled '>20D'. **C,** Modelled (GNOME) quantities of oil beached at 20 days after the initial oil leak, for constant wind conditions. Circled in red are scenarios with (A) the most common wind condition, (B) the shortest time of arrival and (C) the largest quantity of beached oil. Maps of the circled scenarios in Panels B and C are shown in Figure 8. Panels **D** and **E** are for the same wind conditions as in panels B and C, but have been modelled without including the effect of tides.

effect of winds and tides and does not include the effect of waves and surf-zone currents, so was unable to resolve these finer-scale features.

Preliminary analysis of oil spill hazard

The results from modelled scenarios indicate that the time taken for the first oil to reach the shore varies between 14 h and more than 20 days (Figure 7). Oil was found to only reach shore within 20 days if there were onshore winds, suggesting that even relatively weak wind-driven currents may provide greater forcing for oil dispersal than tidal currents in the Bay of Plenty. To test the relative importance of tidal currents in determining the hazard, the GNOME scenario modelling was also undertaken without the tidal currents. Interestingly, tidal currents were found to have an important effect, particularly during periods with low onshore winds, causing the first arrival of oil at the Bay of Plenty shoreline to occur at least 3 days earlier when tidal currents were included (Figure 7D–E).

Scenarios including tidal currents with moderate-high (7–9 m s^{-1}) wind speeds from 340° (NNW) had shorter times to first arrival at the shoreline compared with other

onshore wind scenarios of the same wind speed due to some of the initial oil leaked being transported directly on to Mōtītī Island rather than more typically around the island. The wind in early October 2011 varied in direction (Figure 5A) and so the scenarios modelled in Figure 7 represent the most (onshore winds only) and least (offshore winds only) hazardous end member cases. The case associated with the least beached oil had weak (1 m s^{-1}) winds travelling nearly parallel to the shoreline (100° and 340° or ESE and NNW, respectively) which had the effect of extending the plume alongshore. In the case of higher wind speeds (11 m s^{-1} and greater) and a NNW wind, most of the beached oil on Mōtītī Island was refloated on the leeward side and hence only 91 metric tons was measured.

Figure 8 shows three examples of predicted oil dispersal after the first 6 days following the grounding of the *Rena*. In the scenario that was forced by the observed winds (panel A), there were predominantly offshore winds forcing the oil plume away from the shore. A small amount of oil from the initial leak reached the shore on 10 October, consistent with observations (SCAT surveys). Panels B and C show the most hazardous scenarios, which both involved strong (>11 m s^{-1}) onshore (NNE) winds that forced the floating oil towards the southern entrance of Tauranga harbour. All of these scenarios show that the wind conditions that occurred during the *Rena* grounding switched between typical wind conditions that were moderately hazardous, to the extremely low hazard offshore wind conditions. The wind records show that direction switches every 2–4 days (as in Figure 5) are typical of the wind climate around Tauranga. If the *Rena* grounding had occurred during consistent and strong northwesterlies, the impact could have been much greater.

Model performance

The performance of both Delft3D models was generally satisfactory, with water levels, tidal amplitude and phase predicted very well inside and outside the harbour. Tidal phase tended to be slightly under-predicted at the Omokoroa site in the inner harbour, but this discrepancy may be partly caused by the location of the Omokoroa water level recorder in a small channel that was not well represented in the Delft3D model grid (which had a resolution of 200 × 200 m). There was relatively little difference between the 2D and 3D model versions except right at the southern inlet entrance, suggesting

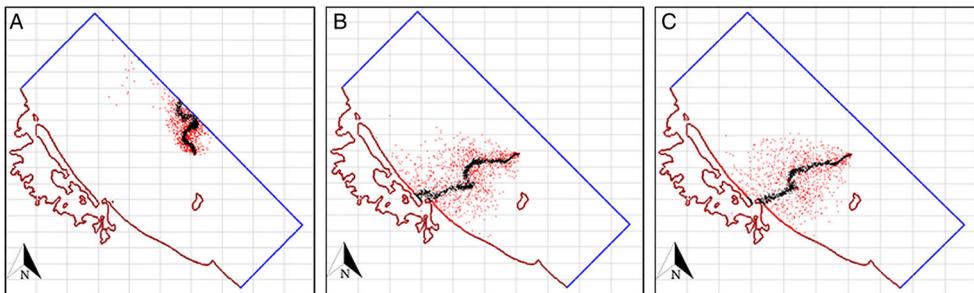**Figure 8.** Maps of modelled (GNOME) oil plumes on 11 October at 2120 h NZST, 6 days after the initial oil leak began, for **A**, recorded wind conditions; **B**, shortest time elapsed for first beaching of oil, and; **C**, largest quantity of beached oil after 20 days. Black dots represent the best guess location of oil particles, while red dots represent the minimum regret positions of oil particles.

that stratification effects are probably not important at this time of the year. This result may not have been the case if the spill had occurred during the summer.

Although current velocity and direction were predicted well at some sites, the model performed less well at predicting current velocity at and just outside the southern Tauranga harbour entrance, with velocity tending to be under-predicted at these sites. A model with a finer grid resolution around Tauranga harbour entrance and tidal channels would probably improve the accuracy of the predicted current velocities. A Delft3D model of the Tauranga harbour southern entrance area (Spiers et al. 2009) achieved an MAE of less than 20% of measured velocities (using the same data set as used for model validation in this study), by increasing grid resolution around the entrance to 2×2 m. However, such a reduction in grid size (the model grid in the current study is 200×200 m) requires a large reduction in the model time step (3 seconds cf. 60 seconds in this study) which leads to a large increase in model run times; simulations covering large areas and time spans are thus rendered largely impractical. In future implementations, further consideration could be given to using a variable grid resolution and more finely resolved bathymetry for areas near harbour entrances, while retaining a coarser grid resolution offshore.

The Delft3D model was forced by tides only, so discrepancies between measured and modelled velocities may be attributable to wind or swell conditions. However, preliminary simulations with wind forcing included in the Delft3D model did not improve model fit, despite the inclusion in the model of finely resolved vertical layers near the surface. Wind forcing was instead included in the GNOME particle tracking model, which included additional parameters for windage and uncertainty, and this inclusion led to improved predictions of oil dispersal and accumulation. The omission of winds in Delft3D may be particularly relevant at sites away from the influence of harbour entrances or tidal channels where tidal forcing may not be the major driver of current velocities, such as at site C1. Although the Bay of Plenty coastline is a typical low-energy wave environment (Heath 1985), it is exposed to swell from the north and northeast that may affect surface currents. Inclusion of, or coupling to, a wave model would increase the complexity (and run times) of the hydrodynamic model, but may improve model performance. We note that GNOME considers only surface oil dispersal and not the dispersal of tar balls and other oil-mineral aggregates that travel deeper in the water column, and so predicted dispersal is particularly sensitive to surface wind conditions. Modelling simulations also did not include shelf currents. It is possible that the relatively enclosed geometry of the Bay of Plenty limited the effect of these kinds of currents and it is likely that performance would not have been so good if the spill had occurred in a much more open location.

Recommendations for oil spill modelling in relation to hazard management

Available data for model calibration and validation comprised sites that were clustered around the Tauranga harbour southern entrance (Figure 2), as the research and monitoring effort had typically been focused on the port and its entrance. The lack of available data for the wider shelf hinders verification of model performance for areas away from Tauranga harbour, but the collection of further hydrodynamic data is outside the scope and resources of this study. This highlights the scarcity of observational data in New Zealand waters that can be used to verify model predictions. Oil dispersal predictions may be highly uncertain if

based on unverified hydrodynamic models. Importantly, this study has highlighted the following critical areas for future research and collaboration:

First, national operational oceanography capability could be improved by ensuring shelf modelling is based on open-source models and freely (and easily) available observations so that uptake of technology is maximised. If agreement were reached on a common open-source model so that bathymetries and boundary files could easily be exchanged between working groups, resources could be utilised much more effectively (in terms of both cost and predictive accuracy of the models) and this would undoubtedly lead to improved hazard management. However, we note that using multiple models to obtain similar results promotes higher levels of confidence in the modelling outcomes.

Second, New Zealand has a scarcity of observational buoys in its waters. Such real-time observations and data assimilative models are vital in order to make accurate real-time modelling forecasts. Such operational forecasts are needed in many situations, from oil spill response to monitoring of harmful algal blooms to search-and-rescue operations. Furthermore, by including measurements from all aspects of the marine environment, not only physical measurements but also biogeochemical and optical water quality measurements, such buoys provide a window to longer-term oceanic changes. Deployment of a number of buoys in key locations and free access to the data would greatly enhance capability for marine environmental prediction. Deploying and maintaining such an observational system is complex, costly and would require multi-organisational cooperation between all interested parties such as government, regional councils, Crown Research Institutes and universities. Consideration should also be given to other monitoring systems, such as high-frequency radar which could be used for operational forecasting of currents around harbour entrances. Such systems provide surface current patterns in real time, over kilometre scales, which can be used to train forecasting models to provide highly accurate results.

Conclusions

The results of this study demonstrate that open-source modelling software (specifically the hydrodynamic model Delft3D and the particle tracking model GNOME) can be used as an effective and relatively low-cost tool to predict oil dispersal. Qualitative comparison of model output with observations of oil accumulation after the *Rena* grounding indicate the GNOME model's ability to predict the first arrival time and the general levels of oil accumulation along the Bay of Plenty coastline. This agreement may have been partly due to the partially enclosed nature of the Bay of Plenty, and modelling of a more open coast location might need to include more open ocean hydrodynamic influences (such as geostrophic currents). Multiple scenarios aimed at understanding the likely hazard associated with a grounding on the Astrolabe Reef highlight the important role of wind strength and direction in determining the likely severity of the outcome. The orientation of the Bay of Plenty coastline makes the area particularly susceptible to wind events from the northeast and north. However, these winds are less common than winds from the southwest.

This study also highlights critical limitations in current capabilities for oil dispersal modelling in New Zealand. For example, the lack of validation data for offshore currents and winds and the lack of a common modelling framework (ideally open-source) for all

institutes that are likely to be involved in any early-response efforts. Such a common modelling system would allow the necessary model set-up parameters to be easily transferred between all working groups. This approach would allow resilience to issues such as variations in the capability of each working group over time owing to personnel changes and absences. New Zealand has a disproportionally large coastal ocean to manage with a small pool of science experts and hence the ability to transfer knowledge and resources quickly is the key to fast and efficient response times.

Acknowledgements

Disclosure statement

Phil Ross is a Research Fellow at the University of Waikato. During the time that this research was conducted, Ross was contracted both by the Bay of Plenty Regional Council and by the owner (Daina Shipping Co.) and insurer (P & I Services) of the MV *Rena* to conduct environmental monitoring and report on monitoring results. Ross was called as an expert witness for the owner and insurer of the MV *Rena* at the Resource Consent hearing in November 2015.

Funding

References

Black KP, Beamsley B, Longdill PC, Moores A. 2005. Bay of Plenty current and temperature measurements: aquaculture management areas, data report. Report for Environment Bay of Plenty. Raglan, New Zealand: ASR Ltd.

Dancuk SN. 2009. The fate and transport of light petroleum hydrocarbons in the lower Mississippi River delta [PhD thesis]. Baton Rouge, LA: Louisiana State University.

Deltares. 2011. Delft3D-FLOW: simulation of multi-dimensional hydrodynamics flows and transport phenonmena, including sediments. User manual version 3.15. The Netherlands: Deltares.

Elias EPL, Walstra DJR, Roelvink JA, Stive MJF, Klein MD. 2000. Hydrodynamic validation of Delft3D with field measurements at Egmond. In: Ledge BL, editor. Proceedings of the 27th International Conference on Coastal Engineering (ICCE); 16–21 July 2000; Sydney, Australia. Reston, VA: American Society of Civil Engineers (ASCE); p. 2714–2727.

Gorman RM, Bryan KR, Laing AK. 2003. A wave hindcast for the New Zealand Region:nearshore validation and coastal wave climate. New Zeal J Mar Freshwat Res. 37:567–588.

Heath RA. 1985. A review of the physical oceanography of the seas around New Zealand — 1982. New Zeal J Mar Freshwat Res. 19:79–124.

Kwoll E. 2010. Evaluation of the Tauranga Harbour numerical model [MSc thesis]. Germany: University of Bremen.

Lesser GR, Roelvink JA, van Kester JATM, Stelling GS. 2004. Development and validation of a three-dimensional morphological model. Coast Eng. 51:883–915.

Longdill PC, Healy TR, Black KP. 2008. Transient wind-driven coastal upwelling on a shelf with varying width and orientation. New Zeal J Mar Freshwat Res. 42:181–196. doi:10.1080/00288330809509947.

Maritime New Zealand. 2011. *Rena* rounding timeline [Internet]. Wellington: Martime New Zealand; [cited 2014 Dec 1]. Available from: http://www.maritimenz.govt.nz/Rena/

Mullarney JC, Hay AE, Bowen AJ. 2008. Resonant modulation of the flow in a tidal channel. J Geophys Res. 113(C10007). doi:10.1029/2007JC004522.

Pawlowicz R, Beardsley B, Lentz S. 2002. Classical tidal harmonic analysis including error estimates in MATLAB using T_TIDE. Comput Geosci. 28:929–937.

Schiel DR, Ross PM, Battershill CN. 2016. Environmental effects of the MV *Rena* shipwreck: cross-disciplinary investigations of oil and debris impacts on a coastal ecosystem. New Zeal J Mar Freshwat Res. 50:1–9.

Soulsby R. 1997. Dynamics of marine sands: a manual for practical applications. London: Thomas Telford Publications Ltd.

Spiers KC, Healy TR, Winter C. 2009. Ebb-jet dynamics and transient eddy formation at Tauranga harbour: implications for entrance channel shoaling. J Coast Res. 251:234–247.

Stephens SA, Healy TR, Black KP, de Lange WP. 1999. Arcuate duneline embayments, infragravity signals, rip currents and wave refraction at Waihi beach, New Zealand. J Coast Res. 15:823–829.

Zelenke B, O'Connor C, Barker C, Beegle-Krause CJ, Eclipse L, editors. 2012. General NOAA operational modeling environment (GNOME) technical documentation. US Department of Commerce, NOAA Technical Memorandum NOS OR&R 40. Seattle, WA: Emergency Response Division, NOAA; [cited 2016 Jan 27]. Available from: http://response.restoration.noaa.gov/gnome_manual

Appendix 1

Table A1.1 Statistical comparison of measured and Delft3D modelled water levels, tidal amplitude and phase.

Site	Calibration or Validation	Water levels		Tidal constituents										
		R^2	MAE (m)	M2 amp error (m)	M2 phase error (°)	N2 amp error (m)	N2 phase error (°)	S2 amp error (m)	S2 phase error (°)	K1 amp error (m)	K1 phase error (°)	O1 amp error (m)	O1 phase error (°)
A Beacon	Calibration	0.982	0.072	−0.01	−1.42	−0.01	1.29	0.01	4.77	−0.01	3.67	−0.01	8.26
Tug Berth	Calibration	0.971	0.078	0.03	−5.64	0.01	−3.69	0.02	1.19	−0.01	0.39	−0.01	9.93
Sulphur Point	Calibration	0.974	0.082	−0.01	−4.53	−0.01	−3.82	0.03	−1.24	−0.01	−15.46	0.01	2.89
Omokoroa	Calibration	0.965	0.082	−0.01	−6.73	−0.01	−6.56	0.03	−6.36	−0.01	−14.68	0.01	17.02
C1	Validation	0.968	0.077	−0.04	−4.23	0.01	1.95	0.03	−0.28	−0.02	−11.77	0.01	13.48
C2	Validation	0.965	0.078	−0.03	−3.89	0.02	2.45	0.03	0.79	−0.02	−13.48	0.01	15.23
C3	Validation	0.965	0.077	−0.02	−4.25	0.02	1.91	0.03	−0.37	−0.02	−13.61	0.01	16.54
C5	Validation	0.958	0.082	0.00	−6.20	0.03	1.34	0.03	−2.45	−0.02	−14.42	0.01	16.61

Notes: MAE, mean absolute error. R^2 is the coefficient of determination.

Table A1.2 Statistical comparison of measured and modelled (Delft3D) current speed and direction.

Site	Calibration or Validation	Tide	Speed (m s^{-1})			Direction (degrees)		
			Mean$_{obs}$	Mean$_{mod}$	MAE	Mean$_{obs}$	Mean$_{mod}$	MAE
ADCP	Calibration	Total	1.10	0.72	0.41			
		Flood	1.10	0.72	0.33	145.77	163.88	18.11
		Ebb	1.48	0.85	0.61	8.00	337.19	30.48
C1	Validation	Total	0.06	0.02	0.04			
		Flood	0.05	0.02	0.04	240.41	239.51	13.70
		Ebb	0.02	0.02	0.01	66.28	64.48	9.13
C2	Validation	Total	0.19	0.10	0.10			
		Flood	0.12	0.07	0.06	213.19	205.17	13.31
		Ebb	0.29	0.14	0.22	20.71	21.33	11.17
C3	Validation	Total	0.16	0.06	0.10			
		Flood	0.12	0.06	0.05	178.40	174.57	13.02
		Ebb	0.23	0.09	0.21	334.05	335.48	10.86
C5	Validation	Total	0.45	0.41	0.10			
		Flood	0.47	0.35	0.10	278.54	265.47	12.82
		Ebb	0.55	0.50	0.08	88.02	87.11	3.52

Notes: MAE, mean absolute error. Mean$_{obs}$ is the mean of the measurements and Mean$_{mod}$ is the mean of the model output.